

# New magnetic intermediate state, “*B-phase*,” in the cubic chiral magnet MnSi

Cite as: APL Mater. 10, 041104 (2022); <https://doi.org/10.1063/5.0084342>

Submitted: 05 January 2022 • Accepted: 08 March 2022 • Published Online: 04 April 2022

 M. Ohkuma,  M. Mito,  M. Pardo, et al.



View Online



Export Citation



CrossMark

## ARTICLES YOU MAY BE INTERESTED IN

[Finding order in disorder: Magnetic coupling distributions and competing anisotropies in an amorphous metal alloy](#)

APL Materials 10, 041103 (2022); <https://doi.org/10.1063/5.0078748>

[Gate control of interlayer exchange coupling in ferromagnetic semiconductor trilayers with perpendicular magnetic anisotropy](#)

APL Materials 10, 041102 (2022); <https://doi.org/10.1063/5.0079245>

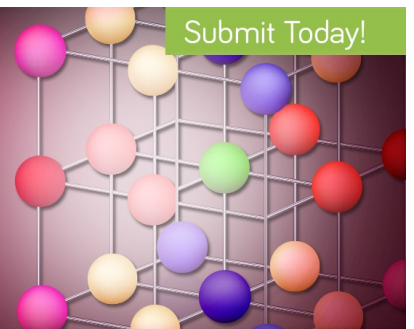
[What controls electrostatic vs electrochemical response in electrolyte-gated materials? A perspective on critical materials factors](#)

APL Materials 10, 040901 (2022); <https://doi.org/10.1063/5.0087396>

**APL Materials**

**Special Topic:** Design and  
Development of High Entropy Materials

Submit Today!



# New magnetic intermediate state, “B-phase,” in the cubic chiral magnet MnSi

Cite as: APL Mater. 10, 041104 (2022); doi: 10.1063/5.0084342

Submitted: 5 January 2022 • Accepted: 8 March 2022 •

Published Online: 4 April 2022



View Online



Export Citation



CrossMark

M. Ohkuma,<sup>1</sup> M. Mito,<sup>1,2,a)</sup> M. Pardo,<sup>3,4</sup> Y. Kousaka,<sup>2,5</sup> S. Iwasaki,<sup>6</sup> K. Ohishi,<sup>7</sup> J. Akimitsu,<sup>6</sup> K. Inoue,<sup>2,8,9</sup> V. Laliena,<sup>10</sup> and J. Campo<sup>2,3,b)</sup>

## AFFILIATIONS

<sup>1</sup> Graduate School of Engineering, Kyushu Institute of Technology, Kitakyushu 804-8550, Japan

<sup>2</sup> Chirality Research Center, Hiroshima University, Higashihiroshima 739-8526, Japan

<sup>3</sup> Aragón Nanoscience and Materials Institute (CSIC–University of Zaragoza) and Physics Condensed Matter Department, Science Faculty, C/ Pedro Cerbuna 12, 50009 Zaragoza, Spain

<sup>4</sup> Graduate School of Science, Osaka Prefecture University, 1-1 Gakuencho, Sakai, Osaka 599-8531, Japan

<sup>5</sup> Department of Physics and Electronics, Osaka Prefecture University, 1-1 Gakuencho, Sakai, Osaka 599-8531, Japan

<sup>6</sup> Research Institute for Interdisciplinary Science, Okayama University, Okayama 700-8530, Japan

<sup>7</sup> Neutron Science and Technology Center, Comprehensive Research Organization for Science and Society (CROSS), Tokai, Ibaraki 319-1106, Japan

<sup>8</sup> Graduate School of Science, Hiroshima University, Higashihiroshima 739-8526, Japan

<sup>9</sup> Institute for Advanced Materials Research, Hiroshima University, Higashihiroshima 739-8526, Japan

<sup>10</sup> Department of Applied Mathematics, University of Zaragoza, C/ María de Luna 3, 50018 Zaragoza, Spain

<sup>a)</sup> Electronic mail: [mitoh@mns.kyutech.jp](mailto:mitoh@mns.kyutech.jp)

<sup>b)</sup> Author to whom correspondence should be addressed: [javier.campo@csic.es](mailto:javier.campo@csic.es)

## ABSTRACT

It is well known that the archetype chiral magnet MnSi stabilizes a skyrmion lattice, termed “A-phase,” in a narrow temperature range in the vicinity of the paramagnetic boundary around  $T_c \sim 29$  K and  $H_c \sim 2$  kOe. Recently, it has been predicted that at much lower temperatures below  $T_c$ , the conical helicoid and the forced ferromagnetic (FFM) states could be separated by a new “unknown state.” In order to detect this “unknown state,” we explored the phase diagram of MnSi oriented single crystals as a function of the d.c. magnetic field ( $\vec{H}_{dc}$ ) and the temperature ( $T$ ) by using a.c. magnetization measurements. For  $\vec{H}_{dc} \parallel \langle 111 \rangle$ , we observed a new region, termed “B-phase,” in the magnetic phase diagram, characterized by a flat-valley-like anomaly on the in-phase component of the a.c. magnetization ( $m'$ ), over  $3.5 \leq H_{dc} \leq 6.2$  kOe just below the low temperature ( $T < 6$  K) FFM boundary. The observed frequency independence over 0.3–1000 Hz and the absence of any measurable absorption in the a.c. magnetization ( $m''$ ) in the “B-phase” suggest a static nature. The “B-phase” was not observed for either  $\vec{H}_{dc} \parallel \langle 100 \rangle$  or  $\langle 110 \rangle$ , revealing that the magnetic anisotropy could play a role in the stabilization of the phase. The “B-phase” could be compatible with the theoretical predictions if the new magnetic state is supposedly related with a relative reorientation of the four helices in MnSi.

© 2022 Author(s). All article content, except where otherwise noted, is licensed under a Creative Commons Attribution (CC BY) license (<http://creativecommons.org/licenses/by/4.0/>). <https://doi.org/10.1063/5.0084342>

Chiral magnets are very promising building blocks for designing new spintronic devices since they can host magnetic textures protected by topology that can be controlled by magnetic fields or electric currents, which made them excellent candidates for a new generation of smart and more efficient spintronics.<sup>1–4</sup> On the other

hand, besides the applications to spintronics, chiral magnets are interesting from a fundamental point of view because the chiral symmetry and its breaking and restoration are ubiquitous phenomena appearing virtually in any domain of science, from particle physics to astrophysics, including chemistry, biology, and geology.<sup>5</sup>

The Dzyaloshinskii–Moriya (DM) interaction,<sup>6–8</sup> present in non-centrosymmetric magnetic materials, often leads to the formation of canted or helimagnetic structures depending on the DM vector ( $\vec{D}_{ij}$ ). In any case, the canting and the pitch angle depend on the competition between the exchange ( $J_{ij}$ ) and the DM ( $D_{ij}$ ) interactions. In helical monoaxial magnets, for which the strong magnetic anisotropies fix the helical axis along a unique crystallographic axis, several magnetic structures (chiral soliton lattices, helical, and conical) can appear, depending on the orientation of the applied magnetic field with respect to the helical axis which, for large enough magnetic fields, end up in a forced ferromagnetic (FFM) phase.<sup>8–12</sup>

In cubic helimagnets, such as the B20 chiral magnet MnSi, in which the DM interaction occurs along three directions, helical structures were found long time ago.<sup>13</sup> Moreover, several decades ago, skyrmion lattices (SkLs) were predicted to appear in cubic magnets under the applied magnetic field,  $\vec{H}_{dc}$ .<sup>14–16</sup> These predictions were corroborated when Mühlbauer *et al.* interpreted the “A-phase” observed in MnSi<sup>17</sup> as a hexagonal SkL phase.<sup>18</sup> Since then, the SkL was subsequently observed in other B20-type alloys,<sup>18–21</sup> multiferroic materials, such as Cu<sub>2</sub>OSeO<sub>3</sub>,<sup>22</sup> and Co–Zn–Mn compounds with the  $\beta$ -Mn structure.<sup>23</sup> Typically, these SkLs are observed in the vicinity of the paramagnetic boundary of the magnetic phase diagram ( $H_c - T_c$ ), and it has been proposed to be stabilized by thermal fluctuations.<sup>18,24</sup> It has also been argued that a combined effect of induced uniaxial anisotropies and applied magnetic fields could stabilize a SkL in cubic helimagnets [e.g., MnSi, FeGe, and (Fe,Co)Si].<sup>25–27</sup>

A few years ago, Laliena and Campo theoretically investigated the instability of the skyrmion textures and the important role of the thermal fluctuations in cubic helimagnets.<sup>28</sup> In fact, it was demonstrated that at zero temperature (T) the only stable phases were the conical helix (CH) and the FFM. Moreover, it was also found that a skyrmionic “A-phase” might exist at low temperatures. They also predicted that a new “unknown state,” surrounded by the FFM, the CH, and the possible new low  $T$  “A-phase,” might emerge in the low temperature region of the phase diagram.

Nakajima *et al.* explored the phase diagram of MnSi by performing small angle neutron scattering (SANS) measurements in equilibrium and also by doing fast quenching from the paramagnetic state to the low  $T$  region, cooling down through the well-known “A-phase” with  $\vec{H}_{dc} \parallel \langle 001 \rangle$ .<sup>29,30</sup> Metastable “A-phase” states were captured at low  $T$  in those experiments, in reasonable agreement with Ref. 28.

New magnetic states, located between the CH and the FFM states at low temperatures, were also reported in the insulator multiferroic Cu<sub>2</sub>OSeO<sub>3</sub> for magnetic fields applied parallel to the  $\langle 100 \rangle$  axis. One of them was recognized to be a skyrmionic state unrelated to the conventional SkL state, and the other was recognized to be a tilted CH state with a propagation vector not aligned with the magnetic field.<sup>31–34</sup>

In Co<sub>7</sub>Zn<sub>7</sub>Mn<sub>6</sub>, in addition to a conventional SkL phase, just below  $T_c$ , a three-dimensionally disordered skyrmion state, stabilized by spin frustration, was also observed.<sup>32,35</sup>

In the recent report on the archetypical cubic helimagnet MnSi, for  $\vec{H}_{dc} \parallel \langle 110 \rangle$ , no new phase has been found.<sup>36</sup> However, the existence of the new low  $T$  phases, “A-phase,” and “unknown state” in

MnSi predicted in Ref. 28 but never observed in this material is still an open question.

This article addresses that open question by carrying out a.c. magnetization experiments in three oriented MnSi enantiopure crystals as a function of  $\vec{H}_{dc}$ ,  $T$ , and frequency ( $f$ ) to carefully explore the low  $T$  region of the phase diagram for each main crystallographic direction. We clearly see that the  $\vec{H}_{dc}$  dependence of a.c. magnetization presents a small flat-valley close to the FFM boundary at low  $T$ , well below  $T_c$ , suggesting the existence of a new “B-phase” that might correspond to the predicted “unknown state.”

Several single crystals of MnSi were synthesized by Bridgman and floating zone methods.<sup>37</sup> They were oriented, with x-ray Laue methods, along the three main cubic axes,  $\langle 100 \rangle$ ,  $\langle 110 \rangle$ , and  $\langle 111 \rangle$ , with sizes of  $3.1 \times 1.1 \times 0.6 \text{ mm}^3$ ,  $2.8 \times 1.1 \times 1.1 \text{ mm}^3$ , and  $2.1 \times 0.5 \times 0.6 \text{ mm}^3$  for, respectively, samples labeled A, B, and C. Some experiments were also performed with the sample B oriented along the  $\langle 111 \rangle$  direction.

In-phase ( $m'$ ) and out-of-phase ( $m''$ ) components of the a.c. magnetization were measured using a superconducting quantum interference device (SQUID) magnetometer, manufactured by Quantum Design. The main frequency  $f$  and the a.c. amplitude were 10 Hz and 3.9 Oe, respectively. In some experiments,  $f$  was varied between 0.3 and 1000 Hz. The experiments were conducted with increasing and decreasing  $H_{dc}$  at fixed temperature below  $T_c$ , after the zero-field cooling procedure from the paramagnetic phase ( $T > T_c = 29.5 \text{ K}$ ). To ensure thermal equilibrium conditions any time, the cooling rate to the target temperature was as slow as 1.5 K/min. Figure 1(a) shows the  $H_{dc}$  dependence of  $m'$  at 2 K for  $\vec{H}_{dc} \parallel \langle 100 \rangle$ ,  $\langle 110 \rangle$ , and  $\langle 111 \rangle$ . For the three samples, the onsets of the CH and FFM phases are clearly observed at  $\sim 1$  and  $\sim 6.5$  kOe, respectively. However, looking carefully at the curves [see Fig. 1(b)], a small anomaly is clearly observed only for sample C, which is oriented with  $\vec{H}_{dc} \parallel \langle 111 \rangle$ , between  $\sim 3.5$  and  $\sim 6.2$  kOe. Indeed, this anomaly has not been detected in the  $H_{dc}$  derivative of d.c. magnetization  $M$  at 2 K for each crystal orientation, as shown in Fig. 1 of the supplementary material. To discard any spurious sample effect, we repeated the same measurements in sample B, but now oriented with the  $\vec{H}_{dc} \parallel \langle 111 \rangle$  axis. In both samples, with the same orientation, we observe the same anomaly, as depicted in Fig. 2(a). The difference observed between both samples is probably due to the different demagnetization field effects in each sample.

Moreover, the “A-phase,” typically observed in the vicinity of the paramagnetic boundary  $T_c$  in MnSi, is clearly observed in our curves of  $m'$  and  $m''$  measured at  $\sim 29 \text{ K}$ , as, respectively, a down pocket and a sharp peak, both arising at  $\sim 1.7$  kOe, for all the three orientations. It is depicted in Figs. 1(c) and 1(d) for sample C, oriented with  $\vec{H}_{dc} \parallel \langle 111 \rangle$ . This is in agreement with the previously reported results for the “A-phase” in MnSi.<sup>38,39</sup> However, the new low  $T$  anomaly does not show any signal in the  $m''$  taken at 2 K, which seems to indicate that the nature of this new state is not skyrmionic [Fig. 1(d)]. This behavior is a first indication about the existence of a new state at low temperatures, just below the FFM state, when the magnetic field is oriented along the  $\langle 111 \rangle$  easy axis. In Cu<sub>2</sub>OSeO<sub>3</sub>, new low  $T$  phases also appeared only for magnetic field directions parallel to its easy axis ( $\langle 100 \rangle$ ).

In sample B oriented with the magnetic field  $\vec{H}_{dc} \parallel \langle 111 \rangle$ ,  $m'$  was measured at 2 K by increasing and decreasing the field from  $0 \rightarrow 8 \rightarrow 0$  kOe. The detail of the new anomaly in  $m'$  is shown in

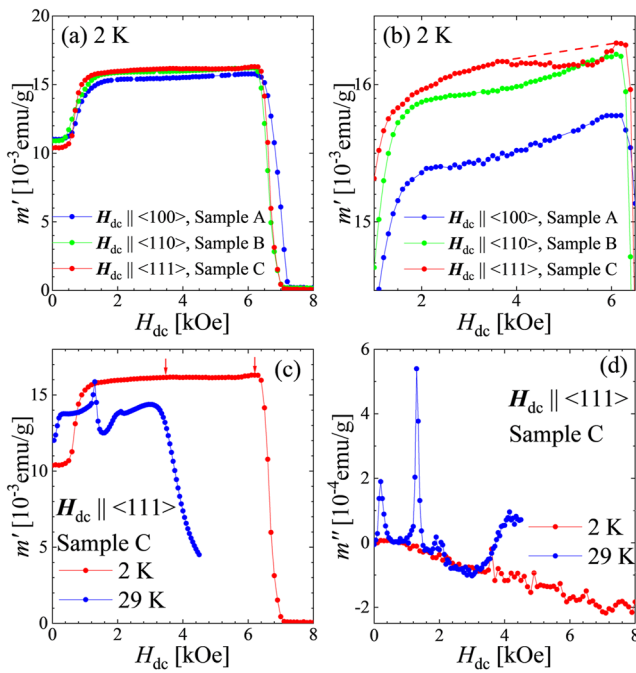


**FIG. 1.** (a)  $H_{dc}$  dependence of  $m'$  at 2 K for  $\vec{H}_{dc} \parallel \langle 100 \rangle$ ,  $\langle 110 \rangle$ , and  $\langle 111 \rangle$  after zero-field cooling. (b) Zoomed region where an anomaly is observed only for sample C. The magnetic field dependence of both in-phase  $m'$  (c) and out-of-phase  $m''$  (d) susceptibilities on MnSi at 2 K (red) and 29 K (blue) is also depicted for  $\vec{H}_{dc}$  applied along the  $\langle 111 \rangle$  direction. The red down arrows in (c) represent that the region of novel state emerges.

Fig. 2(b). The absence of any detectable hysteresis might suggest a continuous phase transition. The contrary happens in  $\text{Cu}_2\text{OSeO}_3$ , where a remarkable hysteresis is present in its new low  $T$  SkL phases. The inset in Fig. 2(b), where the full magnetic field cycle is displayed, shows the hysterical behavior at the low field region due to the single domain formation.

Curves of  $m'$  vs  $H_{dc}$  have been measured at several temperatures in the interval 2–8 K for the three orientations. The anomaly

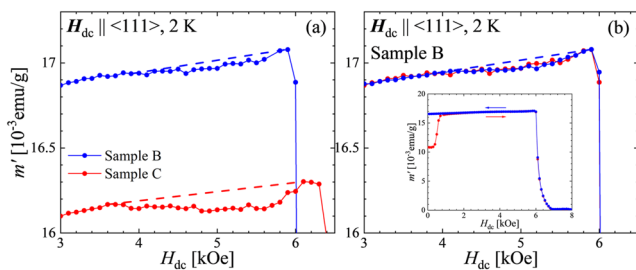


**FIG. 2.** (a) Details of the  $H_{dc}$  dependence of  $m'$  on samples B and C taken at 2 K and with  $\vec{H}_{dc}$  applied along  $\langle 111 \rangle$ . (b) For sample B, details of  $m'$  recorded with increasing (red) and decreasing (blue)  $H_{dc}$  from  $0 \rightarrow 8 \rightarrow 0$  kOe. The dashed line is a guide for the eyes. The inset in (b), where the full magnetic field cycle is displayed, shows the hysterical behavior at the low field region due to the single domain formation.

observed for the crystals oriented along  $\langle 111 \rangle$  at 2 K over  $\sim 3.5$  and  $\sim 6.2$  kOe is disappearing gradually as the temperature increases over  $T \geq 6$  K. These curves are displayed in Fig. 3(a) for sample C. Both the depth and width in the  $m'$  valley decrease with increasing  $T$ , whereas the  $m'$  signal at the bottom ( $\sim 5.5$  kOe) of the  $m'$  valley remains almost constant. This effect is more visible in Fig. 3(c), where a 3D map of the same curves shows a plateau at the top of an  $m'$  mountain. For the other orientations ( $\langle 110 \rangle$  and  $\langle 100 \rangle$ ), where no anomaly is observed at 2 K, a monotonous decreasing of the a.c. signal, as the temperature increases from 2 to 8 K, is observed (see Fig. 2 of the supplementary material).

The new anomaly observed in the curves  $m'$  has been studied at different frequencies ( $f$ ) in the range spanning from 0.3 to 1000 Hz. In this frequency range, the curves do not show any remarkable difference. In the inset of Fig. 3(b), the magnetic field onsets, extracted from the curves measured at 2 K, are displayed for every frequency for sample C, in the field range  $H_{dc}$  covering the region from the CH to FFM states. The characteristic flat-valley defining the anomaly hardly changes against the change in  $f$ . It could suggest that the anomaly is nearly static, without accompanying any energy loss. In addition, a local and continuous rearrangement of the magnetic spin textures could explain these macroscopic frequency independent curves.

We have conducted heat capacity measurements as a function of the temperature in the configuration  $\vec{H}_{dc} \parallel \langle 111 \rangle$ . However, no anomaly was observed in the characteristic  $T$  range where the new

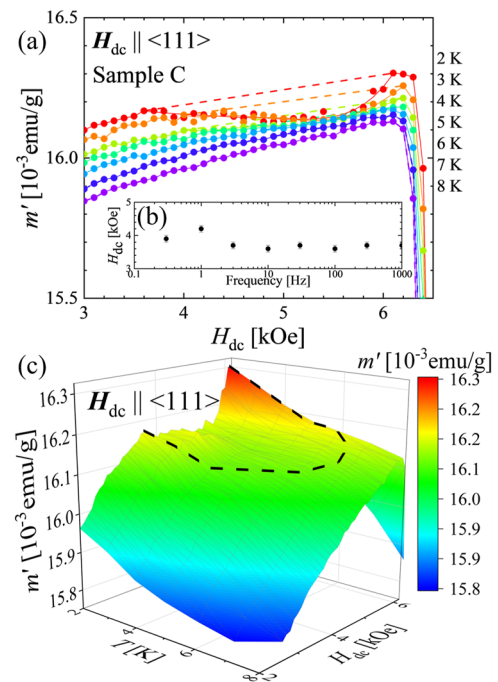


**FIG. 3.** (a)  $H_{dc}$  dependence of  $m'$  at different temperatures measured in sample C. (b) Magnetic field onset for the anomaly, extracted from the curves of  $m'$  at  $T = 2$  K, as a function of the frequency  $f$ . (c) 3D  $m'$  map, below 8 K, for  $\vec{H}_{dc} \parallel \langle 111 \rangle$  covering 2.0–6.2 kOe obtained from  $H_{dc}$ -scanning measurements at a fixed temperature. The dashed line represents the region of the “B-phase.”

state determined by  $m'$  appeared. It could reveal that most of the magnetic entropy is consumed near  $T_c$ , and it hardly survives in the  $H_{dc}$  region near FFM below 7 K.

Collecting all the interesting points from the a.c. magnetization curves vs  $H_{dc}$  and  $T$ , including the points near  $T_c$ , the magnetic phase diagram for MnSi, for  $\vec{H}_{dc} \parallel \langle 111 \rangle$ , is represented in Fig. 4. The typical SkL (“A-phase”) is observed near  $T_c$ . However, at low  $T$ , the CH and FFM phases are present together with a new region, termed “B-phase,” at relatively high magnetic fields. Whereas the typical “A-phase” is observed for the three orientations, (100), (110), and  $\langle 111 \rangle$ , the new “B-phase” is only visible for  $\vec{H}_{dc} \parallel \langle 111 \rangle$ . It should indicate that the cubic magnetic anisotropy terms could play a role, together with the thermal fluctuations, stabilizing such a new state. Our experiments do not detect any anomaly revealing the existence of an equilibrium “A-phase” at low temperatures, which is a hint about the possible metastability of such a phase at low  $T$  observed in Ref. 29. The theoretical developments in Ref. 28 predicted its existence but did not allow us to discern about its metastability.

The MnSi phase diagrams for different orientations of the magnetic field have been the subject of huge interest.<sup>13,25–27,36,38,40–45</sup> However, the focus of those studies was put onto the conventional “A-phase” and onto the low field region ( $H \leq 3.5$  kOe) for a few high symmetry directions, therefore skipping the vicinity of the FFM boundary at low  $T$  ( $T \leq 10$  K). To our best knowledge, this is the first experimental report focusing on the low  $T$  and high magnetic field regime ( $H \geq 3.5$  kOe) in MnSi.

As it has been mentioned before, new low  $T$  phases have been described in the phase diagram of  $\text{Cu}_2\text{OSeO}_3$  oriented crystals along (100). However, the “B-phase,” described in this article, shows very important differences. In MnSi, this “B-phase” does show neither hysteretic behavior with the magnetic field nor any measurable signal in the out-of-phase component of the a.c. magnetization. In addition, in MnSi, the “B-phase” appears when the magnetic field is applied along the main cubic diagonal  $\langle 111 \rangle$ . Moreover, very recent SANS experiments performed in the region where the

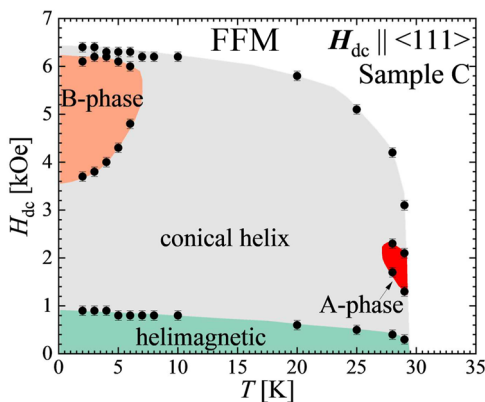


**FIG. 4.** Magnetic phase diagram for the MnSi single crystal for  $\vec{H}_{dc} \parallel \langle 111 \rangle$  deduced from characteristic points of  $m'$  measured vs temperature and magnetic field.

“B-phase” appears showed the typical imprint of a CH phase without any detectable change neither in the modulus of the wave-vector nor in its direction. However, in those experiments, it is a measurable departure from the linear decrease in the integrated intensity of the peaks as the magnetic field increases from  $\sim 3.5$  to  $\sim 6.2$  kOe at 2 K, as reproduced from the [supplementary material](#) of Ref. 46. All these facts together suggest a very different nature for the “B-phase” compared with any typical SkL or tilted CH phases. However, at this moment, our macroscopic and SANS data cannot provide further details about the microscopic nature of such a phase.

To explain the existence of the new low  $T$  magnetic “B-phase” found in MnSi, several mechanisms are available. In 2017, Laliena and Campo studied the stability of the different stationary points (SkL, CH, and FFM) and the role of the thermal fluctuations in cubic chiral magnets, in the low temperature region of the phase diagram,<sup>28</sup> and in the paramagnetic boundary.<sup>24</sup> Such a general micro-magnetic model predicted the existence of a region at low  $T$ , in which all the well-known above-mentioned stationary points are unstable, and therefore, a new magnetic stable “unknown state” should appear in such a region. In addition, in that model, a conventional SkL phase could be present at low  $T$ , as discussed in the precedent paragraphs. That model did not include either any change in the modulus of the magnetic moment or any extra magnetic anisotropy term in its Hamiltonian, necessary to explain the anisotropic behavior observed for the new “B-phase.” However, it is expected that the effect of a very weak magnetic anisotropy, related with the real cubic symmetry, would split the intrinsic degeneracy of the model between the three main cubic directions.

Other theoretical mechanisms, in micromagnetic models at  $T = 0$ , based on the competition of magneto-crystalline anisotropies, but without considering the crucial role of the thermal fluctuations effect in the free energy, are invoked to explain the existence of the new states (SkL and tilted CH phases) observed in  $\text{Cu}_2\text{OSeO}_3$  at low  $T$ .<sup>31,32,47</sup> It is clear that anisotropies must be present because the new states in  $\text{Cu}_2\text{OSeO}_3$  and the new “B-phase” in MnSi appear only for specific directions of the crystal, namely, the anisotropy axis, which are, respectively,  $\langle 100 \rangle$  and the  $\langle 111 \rangle$ . However, it is not still clear which is its hierarchy of energy scales. Moreover, the present observations reveal that the “B-phase” exists even in a system with a very weak magnetic anisotropy, such as MnSi, compared with the related compounds  $\text{Cu}_2\text{OSeO}_3$  or  $\text{Fe}_{1-x}\text{Co}_x\text{Si}$  ( $x = 0.2$ ).<sup>32</sup>

All the mentioned micromagnetic theoretical models have in common the fact that they are not taking into account the local details of the magnetic structure because they consider the density energy in the continuum approximation with a constant averaged magnetic moment.

However, in MnSi (space group  $P2_13$  No. 198), there are four Mn atoms in the  $4a$  Wyckoff position  $(x, x, x)$ , with  $x = 0.138$ , located in the vertices of a tetrahedron.<sup>13</sup> Each one of these Mn develops a helix, all with the same wave-vector  $(\delta, \delta, \delta)$ , with  $\delta \sim 0.035 \text{ \AA}^{-1}$ , therefore producing a given averaged magnetic moment that develops itself a helix with the same wave-vector. Moreover, the symmetry analysis of the magnetic structure for the wave-vector  $(\delta, \delta, \delta)$  and the space group  $P2_13$  in MnSi splits the  $4a$  Wyckoff position in two orbits formed by  $(x, x, x)$  in one orbit and

the three other symmetry equivalents in the other. It allows three different magnetic modes, labeled  $\Gamma_1, \Gamma_2, \Gamma_3$ . For the site  $(x, x, x)$ ,  $\Gamma_1$  describes a magnetic moment pointing in the  $\langle 111 \rangle$  direction, whereas in  $\Gamma_2$  and  $\Gamma_3$ , the magnetic moment lies down in the perpendicular direction. In the other orbit, the symmetry only imposes that the magnetic moments must be related by  $2\pi/3$  or  $4\pi/3$  rotations for  $\Gamma_1, \Gamma_2, \Gamma_3$ . However, it has been experimentally<sup>48</sup> and theoretically<sup>49</sup> found that the magnetic moments are contained in planes perpendicular to the  $\langle 111 \rangle$  direction adopting a quasi in-phase coupling with a small phase-shift angle between both orbits of  $\sim 2^\circ$ .

What is important for this discussion is the fact that phase-shift angle between both orbits is not fixed by the symmetry, and any variation, with the temperature or the magnetic field, will lead to a change in the modulus of the averaged helimagnetic moment. One qualitative picture about the nature of the “B-phase” could be that the temperature and/or the magnetic field could produce a slight relative reorientation of these four conical helices, without any change in the wave-vector of the magnetic structure, but leading to a change in the modulus of the averaged magnetic moment. This slight reorientation should not affect the entropy or the wave-vector of the magnetic structure, as observed in the SANS experiments, and therefore, the effect in the heat capacity curves should be null.

A possible new stationary point in which the averaged magnetic moment modulus should change due to a relative reorientation of the two orbits (each Mn magnetic moment does not change itself) has not been considered in Ref. 28 and might correspond to the predicted “unknown state,” which should be consistent with the “B-phase” reported here.

In conclusion, this article reports for the first time about the existence of a new magnetic state at low temperatures, the “B-phase,” which spans over a magnetic field range of  $H_{dc}$  of 3.5–6.2 kOe in the archetype cubic chiral magnet MnSi through a.c. magnetization measurements. In contrast to what happens in the “A-phase,” this new phase is only detectable when the field direction is parallel to the  $\langle 111 \rangle$  axis and does not show any detectable energy absorption or frequency dependence. This could be compatible with the predictions in Ref. 28 if the new magnetic state is supposedly related to a relative reorientation of the four helices in MnSi. More experimental and theoretical work giving light about the local details (e.g.,  $\mu$ SR) of the magnetic moments rearrangements is needed to corroborate this possibility.

See the [supplementary material](#) for more details on the magnetization measurements and small angle neutron scattering experiments in MnSi.

This work was funded by MCIN/AEI/10.13039/501100011033 under Grant No. PGC2018099024B100. Grant No. OTR02223 from CSIC/MICIN and Grant No. DGA/M4 from Diputación General de Aragón (Spain) are also acknowledged. This work was supported by Grants-in-Aid for Scientific Research, Grant No. (S) 25220803, from the Ministry of Education, Culture, Sports, Science and Technology (MEXT), Japan; by JSPS KAKENHI under Grant Nos. K16KK0102, H17H06137, K19KK0070, and H20H02642; by the MEXT program for promoting the enhancement of research universities; by the JSPS Core-to-Core Program, A. (Advanced Research Networks); and by the Chirality Research Center (Crescent) in Hiroshima University.

## AUTHOR DECLARATIONS

### Conflict of Interest

The authors have no conflicts to disclose.

### DATA AVAILABILITY

The data that support the findings of this study are available from the corresponding author upon reasonable request.

## REFERENCES

- S. Wolf, D. Awschalon, R. Buhrman, J. Daughton, S. von Molnár, M. Roukes, A. Chtchelkanova, and D. Treger, *Science* **294**, 1488 (2013).
- I. Žutić, J. Fabian, and S. D. Sarma, “Spintronics: Fundamentals and applications,” *Rev. Mod. Phys.* **76**, 323 (2004).
- A. Fert, V. Cros, and J. Sampaio, *Nat. Nanotechnol.* **8**, 152 (2013).
- N. Romming, C. Hanneken, M. Menzel, J. Bickel, B. Wolter, K. von Bergmann, A. Kubetzka, and R. Wiesendanger, *Science* **341**, 636 (2011).
- G. H. Wagniere, *On Chirality and the Universal Asymmetry, Reflections on Image and Mirror Image* (Wiley VCH, Zurich, 2007).
- I. Dzyaloshinskii, *J. Phys. Chem. Solid* **4**, 241–255 (1958).
- T. Moriya, *Phys. Rev.* **120**, 91–98 (1960).
- I. Dzyaloshinskii, *Sov. Phys. JETP* **19**, 960 (1964).
- J.-I. Kishine, K. Inoue, and Y. Yoshida, *Prog. Theor. Phys. Suppl.* **159**, 82–95 (2005).
- V. Laliene, J. Campo, and Y. Kousaka, *Phys. Rev. B* **94**, 094439 (2016).
- V. Laliene, J. Campo, J.-I. Kishine, A. S. Ovchinnikov, Y. Togawa, Y. Kousaka, and K. Inoue, *Phys. Rev. B* **93**, 134424 (2016).
- V. Laliene, J. Campo, and Y. Kousaka, *Phys. Rev. B* **95**, 224410 (2017).
- Y. Ishikawa, K. Tajima, D. Bloch, and M. Roth, *Solid State Commun.* **19**, 525–528 (1976).
- A. N. Bogdanov and D. A. Yablonskii, *Sov. Phys. JETP* **68**, 101 (1989).
- A. Bogdanov and A. Hubert, *J. Magn. Magn. Mater.* **138**, 255–269 (1994).
- A. Bogdanov and A. Hubert, *J. Magn. Magn. Mater.* **195**, 182–192 (1999).
- Y. Ishikawa, G. Shirane, J. A. Tarvin, and M. Kohgi, *Phys. Rev. B* **16**, 4956–4970 (1977).
- S. Mühlbauer, B. Binz, F. Jonietz, C. Pfleiderer, A. Rosch, A. Neubauer, R. Georgii, and P. Boni, *Science* **323**, 915–919 (2009).
- W. Münzer, A. Neubauer, T. Adams, S. Mühlbauer, C. Franz, F. Jonietz, R. Georgii, P. Böni, B. Pedersen, M. Schmidt, A. Rosch, and C. Pfleiderer, *Phys. Rev. B* **81**, 041203 (2010).
- X. Z. Yu, Y. Onose, N. Kanazawa, J. H. Park, J. H. Han, Y. Matsui, N. Nagaosa, and Y. Tokura, *Nature* **465**, 901–904 (2010).
- X. Z. Yu, N. Kanazawa, Y. Onose, K. Kimoto, W. Z. Zhang, S. Ishiwata, Y. Matsui, and Y. Tokura, *Nat. Mater.* **10**, 106–109 (2011).
- S. Seki, X. Z. Yu, S. Ishiwata, and Y. Tokura, *Science* **336**, 198–201 (2012).
- Y. Tokunaga, X. Z. Yu, J. S. White, H. M. Rønnow, D. Morikawa, Y. Taguchi, and Y. Tokura, *Nat. Commun.* **6**, 7638 (2015).
- V. Laliene, G. Albalade, and J. Campo, *Phys. Rev. B* **98**, 224407 (2018).
- M. N. Wilson, A. B. Butenko, A. N. Bogdanov, and T. L. Monchesky, *Phys. Rev. B* **89**, 094411 (2014).
- A. B. Butenko, A. A. Leonov, U. K. Rößler, and A. N. Bogdanov, *Phys. Rev. B* **82**, 052403 (2010).
- H. Wilhelm, M. Baenitz, M. Schmidt, U. K. Rößler, A. A. Leonov, and A. N. Bogdanov, *Phys. Rev. Lett.* **107**, 127203 (2011).
- V. Laliene and J. Campo, *Phys. Rev. B* **96**, 134420 (2017).
- T. Nakajima, H. Oike, A. Kikkawa, E. P. Gilbert, N. Booth, K. Kakurai, Y. Taguchi, Y. Tokura, F. Kagawa, and T.-h. Arima, *Sci. Adv.* **3**, e1602562 (2017).
- T. Nakajima, Y. Inamura, T. Ito, K. Ohishi, H. Oike, F. Kagawa, A. Kikkawa, Y. Taguchi, K. Kakurai, Y. Tokura, and T.-h. Arima, *Phys. Rev. B* **98**, 014424 (2018).

- <sup>31</sup>A. Chacon, L. Heinen, M. Halder, A. Bauer, W. Simeth, S. Mühlbauer, H. Berger, M. Garst, A. Rosch, and C. Pfleiderer, *Nat. Phys.* **14**, 936–941 (2018).
- <sup>32</sup>M. Halder, A. Chacon, A. Bauer, W. Simeth, S. Mühlbauer, H. Berger, L. Heinen, M. Garst, A. Rosch, and C. Pfleiderer, *Phys. Rev. B* **98**, 144429 (2018).
- <sup>33</sup>F. Qian, L. J. Bannenberg, H. Wilhelm, G. Chaboussant, L. M. Debeer-Schmitt, M. P. Schmidt, A. Aqeel, T. T. M. Palstra, E. Brück, A. J. E. Lefering, C. Pappas, M. Mostovoy, and A. O. Leonov, *Sci. Adv.* **4**, eaat7323 (2018).
- <sup>34</sup>L. J. Bannenberg, H. Wilhelm, R. Cubitt, A. Labh, M. P. Schmidt, E. Lelièvre-Berna, C. Pappas, M. Mostovoy, and A. O. Leonov, *npj Quantum Mater.* **4**, 11 (2019).
- <sup>35</sup>K. Karube, J. S. White, D. Morikawa, C. D. Dewhurst, R. Cubitt, A. Kikkawa, X. Yu, Y. Tokunaga, T.-h. Arima, H. M. Rønnow, Y. Tokura, and Y. Taguchi, *Sci. Adv.* **4**, eaar7043 (2018).
- <sup>36</sup>L. J. Bannenberg, F. Weber, A. J. E. Lefering, T. Wolf, and C. Pappas, *Phys. Rev. B* **98**, 184430 (2018).
- <sup>37</sup>Y. Kousaka, N. Ikeda, T. Ogura, T. Yoshii, J. Akimitsu, K. Ohishi, J.-i. Suzuki, H. Hiraka, M. Miyagawa, S. Nishihara, K. Inoue, and J.-i. Kishine, *JPS Conf. Proc.* **2**, 010205 (2014).
- <sup>38</sup>A. Bauer and C. Pfleiderer, *Phys. Rev. B* **85**, 214418 (2012).
- <sup>39</sup>K. Tsuruta, M. Mito, H. Deguchi, J. Kishine, Y. Kousaka, J. Akimitsu, and K. Inoue, *Phys. Rev. B* **97**, 094411 (2018).
- <sup>40</sup>A. I. Okorokov, S. V. Grigoriev, Y. O. Chetverikov, S. V. Maleyev, R. Georgii, P. Böni, D. Lamago, H. Eckerlebe, and K. Pranzas, *Physica B* **356**, 259–263 (2005).
- <sup>41</sup>S. V. Grigoriev, S. V. Maleyev, A. I. Okorokov, Y. O. Chetverikov, R. Georgii, P. Böni, D. Lamago, H. Eckerlebe, and K. Pranzas, *Phys. Rev. B* **72**, 134420 (2005).
- <sup>42</sup>S. V. Grigoriev, S. V. Maleyev, A. I. Okorokov, Y. O. Chetverikov, and H. Eckerlebe, *Phys. Rev. B* **73**, 224440 (2006).
- <sup>43</sup>S. V. Grigoriev, S. V. Maleyev, A. I. Okorokov, Y. O. Chetverikov, P. Böni, R. Georgii, D. Lamago, H. Eckerlebe, and K. Pranzas, *Phys. Rev. B* **74**, 214414 (2006).
- <sup>44</sup>A. Bauer, M. Garst, and C. Pfleiderer, *Phys. Rev. Lett.* **110**, 177207 (2013).
- <sup>45</sup>A. Bauer, A. Chacon, M. Wagner, M. H. Georgii, A. Rosch, C. Pfleiderer, and M. Garst, *Phys. Rev. B* **95**, 024429 (2017).
- <sup>46</sup>K. Ohishi, Y. Kousaka, S. Iwasaki, J. Akimitsu, M. Pardo-Sainz, V. Laliena, J. Campo, M. Ohkuma, and M. Mito, *JPS Conf. Proc.* **33**, 011606 (2021).
- <sup>47</sup>A. O. Leonov, C. Pappas, and I. Kézsmárki, *Phys. Rev. Res.* **2**, 043386 (2020).
- <sup>48</sup>P. Dalmas de Réotier, A. Maisuradze, A. Yaouanc, B. Roessli, A. Amato, D. Andreica, and G. Lapertot, *Phys. Rev. B* **95**, 180403 (2017).
- <sup>49</sup>K. P. W. Hall and S. H. Curnoe, *Phys. Rev. B* **104**, 094408 (2021).